# A modelling approach with Macroscopic Cellular Automata for hazard zonation of debris flows and lahars by computer simulations

Valeria Lupiano, Guillermo Machado, Gino M. Crisci and Salvatore Di Gregorio

***Abstract*—** Cellular Automata (CA) represent both abstract dynamical systems evolving on the base of local interactions of their constituent parts and a parallel computational paradigm for modelling complex phenomena, whose evolution may be explicated mostly in terms of local rules. CA represent a powerful tool for simulating fluid-dynamical system; Macroscopic CA (MCA) characterize a methodological approach, which proved efficacious for modelling and simulating large scale surface flows. Fast-moving flow-like "landslides", as lahars, debris and mud flows, give rise to very destructive natural disasters as number of casualties in the world. Simulation of such phenomena could be an important tool for hazard management in threatened regions. This paper presents the modelling methodology of MCA for such a type of surface flows together with some models, based on this approach. They are SCIDDICA-SS2, SCIDDICA-SS3 (both for debris, mud and granular flows) and LLUNPIY (for primary and secondary lahars). Such models share certain features (common sub-states and elementary processes), while different specifications are introduced according to the peculiarities of related surface flows. Examples of simulations of both past (validation phase) and probable future events (developing hazard scenarios) are presented for each model. The last version of LLUNPIY is here introduced with new applications to lahar hazard related to Ecuador's volcanos Cotopaxi and Tungurahua.

***Keywords*—**Cellular Automata, Debris flow, Lahars, Modeling and Simulation, Natural Hazard.

## I. Introduction

JOHN von Neumann conceived Cellular Automata (CA) at the end of the 1940s on suggestion of Stanislaw Ulam, for the purpose of studying the formal (and computational) properties of self-reproducing organisms, with the most general notion of self-reproduction in mind, to be combined with the notion of universal calculability [1]. Interest in CA by the scientific community had been intermittent, but today they have been firmly established as a parallel calculation model and a tool to model and simulate complex phenomena.

CA are spatially and temporally discrete, abstract computational systems that can exhibit chaotic behavior, self-organization and lend themselves to descriptions in rigorous mathematical terms, these have proven useful both as general models of complexity of non-linear dynamics, in a diversity of scientific fields. The computational model of the growth of a snowflake is an example of the CA. It is represented by a uniform array of numerous identical cells, where each cell may assume only a few states and interact with only a few adjacent cells. The elements of the system (the cells and the rule to calculate the subsequent state of a cell) can be very simple, yet nonetheless give rise to a notably complex evolution [2].

In its essential description, CA can be seen as a space, partitioned in cells, each one embedding an identical input/output computing unit. Each cell is characterized by its state. *S* is the finite set of the states. Input for each cell is local and is given by the states of *m* neighboring cells, where the neighborhood conditions are given by a pattern invariant in time and space. At time 0, cells are in arbitrary states (initial conditions) and the CA evolves changing simultaneously the state at discrete times, according to local evolution rules, which are functions of the states of the cell itself and its neighbors.

Since the self-reproduction application, CA are widely applied to various fields of arts, biology, chemistry, communication, cultural heritage, ecology, economy, geology, engineering, medicine, physics, sociology, traffic control, etc.

In the last years, the research into simulations of CA in fluid dynamics, as an important field for CA applications, is accelerating in many directions. One of the research directions concerns modelling and simulation of flow-type landslides, that have been carried out by several authors with satisfactory results since 1986 [3]. An extension of the CA paradigm for macroscopic systems and a related modeling methodology were established in order to simulate also fluid-dynamical phenomena [4]. Good simulations results were obtained for some types of "macroscopic" surface flows, for instance, lava flows and pyroclastic flows for volcanic eruptions, debris, mud, granular flows for landslides with various versions of the SCIDDICA, SCIARA, PYR and VALANCA models respectively e.g., [5], [6], [7], [8]. Other significant MCA

V. Lupiano is with Dept. of Biology, Ecology, Earth Science, University of Calabria, Arcavacata, 87036 Rende, Italy (corresponding author; phone: +390984493691; fax: +390984493570; e-mail: valeria.lupiano@unical.it).

G. Machado, is with Faculty of Engineering, National University of Chimborazo, 060150 Riobamba, Ecuador, and with Dept. of Mathematics and Computer Science, University of Calabria, Arcavacata, 87036 Rende, Italy (e-mail: gmachado@unach.edu.ec).

G. M. Crisci is with is with Dept. of Biology, Ecology, Earth Science, University of Calabria, Arcavacata, 87036 Rende, Italy (e-mail: crisci@unical.it).

S. Di Gregorio is with Dept. of Mathematics and Computer Science, University of Calabria, Arcavacata, 87036 Rende, Italy (e-mail: salvatore.digregorio@unical.it).

models were developed for flow-type landslides [9], [10].

In this context, the next section considers the MCA general frame for modeling macroscopic surface flow, an extended definition of CA for modeling macroscopic phenomena that can be framed in an acentric context, developing CA alternative strategies, which are reported in the subsequent sections. Afterward, the three cellular models SCIDDICA-SS2 [11], SCIDDICA-SS3 [12] and LLUNPIY [13], [14], concerning respectively debris flows and lahars are exposed together with simulation examples of real cases (validation cases) and simulation applications for developing future probable scenarios (Spatial Decision Systems in order to mitigate natural hazard). Comments and conclusions are reported at the end.

## II. MCA General Frame

The applications of CA to fluid dynamics have generated two important computational paradigms: the *Lattice Gas* models [15], and from there, the more robust *Lattice Boltzmann method* [16], [17]. However, many complex macroscopic phenomena seem to be difficult to model with these types of CA, since they occur on a very broad spatial scale. Consequently, a macroscopic level of description must be used, which implies, however, the management of a large quantity of data, e.g. morphological data. It is hence unthinkable to work at the microscopic or mesoscopic level, where evaluation factors such as data quality would make no sense. The move to the macroscopic level also means a greater number of states, which could also lead to complicated transition functions that can no longer be practically identified with a lookup table, as in the microscopic case.

The classical CA definition is not sufficient for modelling spatially extended natural macroscopic phenomena [18]. This extension in its completeness does not formally alter the classic notion of CA as developed by von Neumann, but renders it capable of modeling and dealing with the complex macroscopic phenomena to be simulated. A very high number of states are needed for macroscopic phenomena, because they must contain all the information related to the portion of space corresponding to the cell, with all the specifications needed to model the evolution of the phenomenon of interest. This gives rise to a very high number of states, which can be formally represented in terms of sub-states (i.e., the Cartesian product of the sets of all the sub-states constitutes the set of the states). In this way, a sub-state specifies important characteristics (e.g., altitude, temperature, etc.) to be attributed to the state of the cell and necessary to determine the evolution of the CA**.**

### *A. CA Criteria for modeling of macroscopic phenomena*

When The extended definition of CA for modeling macroscopic phenomena descends from the need to correlate the evolution of the phenomenon with the evolution of the simulation; it is necessary also to consider, those simple, non-local specifications (the parameters) related to the phenomenon or its representation in terms of CA (Etnean lava solidification temperature, cell dimension, etc.).

A CA is formally defined as a septuplet:

$$\langle R,G,S,X,P,\tau,\gamma \rangle$$

when its components are specified as follows.

- **Global parameters**

The abstract CA must be uniquely related to the real macroscopic phenomena with regard to time and space.

Some global parameters must be considered: at least

• the cell dimensions e.g. the distance between the centers of two neighboring cells $p_d$;

• the time corresponding to one step of the transition function $p_t$;

$P = (p_d, p_t, \ldots.)$ is the finite set of global parameters that affect the transition function.

- **Space**

The cell normally corresponds to a portion of space; therefore, the cellular space should be three-dimensional: $R = \{(x,y,z) \mid x,y,z \in N\}$ with $0 \le x \le l_x$, $0 \le y \le l_y$, $0 \le z \le l_z$, is the set of coordinates integer points that define the finite region of the space where the phenomenon evolves. N is the set of natural numbers.

If there are legitimate simplifications, it is easy to reduce the formula to 1-2 dimensions.

- **Sub-states**

The macroscopic part of the phenomenon may imply heterogeneity. Each characteristic significant to the evolution of the system and related to the portion of space corresponding to the cell is identified as a sub-state; the Cartesian product of the sets of sub-states expresses the finite set S of the states:

$$S= S_1 \times S_2 \times \ldots.. \times S_n$$

The value of a sub-state is approximated to a unique value in the space occupied by the cell (e.g., the temperature).

When a characteristic (e.g., a physical quantity) is expressed as a continuous variable, then a finite but sufficient number of meaningful digits are used so that the set of possible values can be arbitrarily large but finite.

The cellular space should be three-dimensional, but a reduction to two dimensions is permitted if the quantity related to the third dimension (height) can be represented as sub-states of the cell: this is the case with surface flows, which include debris flows, mudflow, granular flows and lahars.

- **"Elementary" Processes**

Just as the state of the cell can be broken down into sub-states, the transition function $\tau$ can be subdivided into "elementary" processes, defined by the functions $\sigma_1, \sigma_2 \ldots . \sigma_k$ with *k* being the number of elementary processes.

The elementary processes are applied sequentially according to a defined order. Different elementary processes can result in a different neighborhood. Each elementary process updates the states of the CA.

- **Neighborhood**

$X=\{\xi_0, \xi_1, \ldots.. \xi_{m-1}\}$, the neighborhood relationship (or index), is a finite set of three-dimensional vectors, that specifies the cells belonging to the neighborhood by addition of co-ordinates of the considered cell, the so called central cell. The union of all neighborhoods associated with each elementary process specifies the CA neighborhood.

- **External influences**

Sometimes, a sort of input from the "external world" on the cells of the *CA* must be considered; these account for external influences that cannot be described in local terms (e.g., the rainfall) for simulating on the base of real or probabilistic data. Therefore, special and/or additional functions ($\gamma$) must be specified for that type of cell ($G$). $\gamma$ and $G$ do not need to be always specified in the CA models.

### *B. Algorithm of Minimization of Differences*

Many complex systems evolve locally toward conditions of maximum possible equilibrium: essentially in terms of *CA*, the system tends to minimize, within the neighborhood, differences related to a certain amount of matter, giving rise to flows from central cell to the other neighbor cells [19], [4].

In the context of *CA*, this means that sub-states "outflow" have to be calculated for the generic cell $c$ from the "distributable" quantity $q_d$. Values of such outflows correspond to values of the sub-states "inflow" for $c$ neighbors in the next step. $\tau$ is applied simultaneously on each cell in $R$ and flows, potentially from each cell toward neighborhood cells, give rise to the evolution of the system.

- Explicatum of the minimization problem

Definitions:

$n = \#X$ ;

$q_d$ = distributable quantity in the central cell;

$q_0$ = not distributable quantity in the central cell;

$q_i$ = quantity in the cell $i$ $1 \le i < n$ ;

$f_0'$ is the part of $q_d$ remaining in the central cell;

$f_i'$ = flow from the central cell towards the cell $i$ $1 \le i < n$ ;

$q_i' = q_i + f_i'$ $0 \le i < n$ ;

*Bound:* $q_d = \Sigma_{0 \le i < n} f_i'$ ;

*Problem:* $f_h'$ $0 \le h < n$ must be determined in order to minimize the sum of all $q$ differences between all the pairs of cells in the neighborhood:

$$\sum_{\{(i,j)|0 \le i < j < n\}} |q_i' - q_j'| \tag{1}$$

- **Minimization of the Differences**

*Initialization:*

a) all the neighboring cells are considered "admissible" to receive flows from the central cell, $A$ is the set of admissible cells.

*Cycle:*

b) the "average $q$" ($av\_q$) is found for the set $A$ of admissible cells:

$$av\_q = (q_d + \Sigma_{i \in A} q_i) / \#A. \tag{2}$$

c) each cell $x$ with $q_x \ge av\_q$ is eliminated from the set $A$. It implies that "average $q$" does not increase, because:

$$av\_q = (q_d + \Sigma_{i \in A} q_i) / \#A =$$
$$= (q_d + \Sigma_{i \in A} q_i - av\_q) / (\#A - 1) \ge \tag{3}$$
$$\ge (q_d + \Sigma_{i \in A} q_i - q_x) / (\#A - 1)$$

*End of cycle:*

d) go to step-b until no cell is eliminated.

*Result:*

e) $f_i' = av\_q - q_i$ for $i \in A$ $(q_i < av\_q)$;
$f_i' = 0$ for $i \notin A$ $(q_i' \ge av\_q)$

*Conservation bound:*

$$\Sigma_{i \in A} f_i' = \Sigma_{i \in A} (av\_q - q_i) = \tag{4}$$
$$= \#A(q_d + \Sigma_{i \in A} q_i) / \#A - \Sigma_{i \in A} q_i = q_d$$

*Properties:*

P1: $q_i' = f_i' + q_i = av\_q - q_i + q_i = av\_q$ for $i \in A$

P2: $q_i' = q_i$ because $f_i' = 0$ for $i \notin A$

### *C. Validation phase of MCA models*

Two main phases are involved for verifying the reliability of MCA simulation models: the calibration phase identifies an optimal set of parameters capable of adequately reproduce the observed event; the validation phase, in which the model is tested on a sufficient (and different) number of cases similar in terms of physical and geomorphologic properties. Once the optimal set of parameters is calibrated, the model can be considered applicable in the same homogeneous geological context in which the parameters are derived, enabling a predictive analysis of surface flow hazard.

The likelihood between the cells involved by the real event and the cells involved in the simulation can be measured by the fitness function in relation to the dimensions $d$ of cellular space:

$$f(R,S) = \sqrt[d]{\frac{R \cap S}{R \cup S}} \tag{5}$$

where $R$ is the set of cells involved in the real event and $S$ is the set of cells involved in the simulated event. This function ranges from **0** (completely wrong simulation) to **1** (perfect match between real and simulated events); values greater than **0.7** may be considered acceptable for two dimensions.

## III. THE MODEL SCIDDICA-SS2

This version of SCIDDICA is an extension of model applied to the landslides of Sarno [20]. Such an extension involves more sub-states, processes and parameters because the phenomenon is more complex [21]. In fact, the most sophisticated version SS2 is shortly presented together with the simulation of the combined subaerial-subaqueous part of Albano landslide (Rome, Italy).

### *A. Main features of SCIDDICA-SS2*

The hexagonal CA model SCIDDICA-SS2 is the quintuple $\langle R, X, S, P, \tau \rangle$:

- $R$ is the set of regular hexagons covering the region, where the phenomenon evolves.
- $X$ identifies the geometrical pattern of cells, which influence any state change of the central cell: the central cell (index 0) itself and the six adjacent cells (indexes 1,…6).
- $S$ is the fine set of states of the fine automaton, it is equal to the Cartesian product of the sets of the considered sub-states (Table I).

- $P$ is the set of global physical and empirical parameters, which account for the general frame of the model and the physical characteristics of the phenomenon (Table II).
- $\tau: S^7 \rightarrow S$ is the deterministic state transition function; its elementary processes are shortly summarized in the next section.

Table I Subs-states

| Sub-states | Description |
|---|---|
| $S_A$, $S_D$ | cell **A**ltitude, the maximum **D**epth of detrital cover. |
| $S_{TH}$ | the average **T**hickness **H**ead of landslide debris inside the cell |
| $S_{KH}$ | the debris **K**inetic **H**ead |
| $S_X$, $S_Y$ | the co-ordinates **X** and **Y** of the lahar barycenter inside the cell |
| $S_E$, $S_{EX}$, $S_{EY}$, $S_{KHE}$ (6 components) | the part of debris flow (**E**xternal flow), **E**xternal flow co-ordinates **X** and **Y**, the debris kinetic head |
| $S_I$, $S_{IX}$, $S_{IY}$, $S_{KHI}$ (6 components) | the part of debris flow toward the adjacent cell (**I**nternal flow), **I**nternal flow co-ordinates **X** and **Y**, **K**inetic **H**ead of **I**nternal flow |

Table II Physical and empirical parameters

| Parameters | Description |
|---|---|
| $p_a$ , $p_t$ | cell **a**pothem, **t**emporal correspondence of a CA step |
| $p_{adhw}$, $p_{adha}$ | the **w**ater/**a**ir **adh**esion values |
| $p_{fcw}$ , $p_{fca}$ | the **w**ater/**a**ir **f**riction **c**oefficient for debris outflows |
| $p_{tdw}$ , $p_{tda}$ $p_{edw}$ , $p_{eda}$ | **w**ater/**a**ir parameters for energy **d**issipation by **t**urbulence and by **e**rosion respectively |
| $p_{ml}$ | the **m**atter **l**oss in percent when the debris enters into water |
| $p_{mtw}$ , $p_{mta}$ | the **w**ater/**a**ir activation **t**hresholds of the **m**obilization |
| $p_{tmt}$ | the activation **t**hreshold of the **m**obilization for the **t**ransept |
| $p_{pew}$ , $p_{pea}$ | the **w**ater/**a**ir **p**rogressive **e**rosion parameters |
| $p_{wr}$ | the **w**ater **r**esistance parameter |

*B. SCIDDICA-SS2 transition function*

Define In the following, a sketch of the local elementary processes will be given, in order to capture the mechanisms of the transition function; the execution of an elementary process updates the sub-states. Variables concerning sub-states and parameters are indicated by their subscript. When sub-states need the specification of the neighborhood cell, their index is indicated between square brackets. $\Delta Q$ means variation of the sub-state $S_Q$.

- **Mobilization effects**

Number When the kinetic head value overcomes an opportune threshold ($KH>mt$) depending on the soil features and its saturation state then a mobilization of the detrital cover occurs proportionally to the quantity overcoming the threshold:

$$pe\cdot(KH-mt) = \Delta TH = -\Delta D \quad (6)$$

(the detrital cover depth diminishes as the debris thickness increases), the kinetic head loss is:

$$-\Delta KH = ed\cdot(KH-mt) \quad (7)$$

- **Turbulence effect**

The effect of the turbulence is modelled by a proportional kinetic head loss at each SCIDDICA step:

$-\Delta KH=td\cdot KH$.

- **Debris outflows**

Outflows computation is performed in two steps: determination of the outflows by the Algorithm for the Minimization of Differences (AMD, [4]) applied to "heights" of the cell neighborhood and determination of the shift of the outflows [18].

SCIDDICA-SS2 involves a type of alteration of data regarding the height values in order to account for run-up effects concerning kinetic energy, expressed by kinetic head.

Terms of AMD are the height ($h$) of cells in the neighborhood, to be minimized by flows ($f$), whose sum is equal to the quantity $q$ to be distributed in the neighborhood cells.

$$h[0] = A[0] + KH[0] + adh \quad (8)$$
$$h[i] = A[i]+TH[i],(1\leq i\leq 6) \quad (9)$$
$$q = TH[0] - adh = \Sigma_{0\leq i\leq 6} f[i] \quad (10)$$

AMD application minimizes

$$\Sigma_{\{(i,j)\,|\,0\leq i<j\leq 6\}}(|(h[i]+f[i]) - (h[j]+ f[j])|) \quad (11)$$

The barycenter co-ordinates $x$ and $y$ of moving quantities are the same of all the debris inside the cell and the form is ideally a "cylinder" tangent the next edge of the hexagonal cell. An ideal distance "$d$" is considered between the central cell debris barycenter and the center of the adjacent cell $i$ including the slope $\theta[i]$.

The $f[i]$ shift "$sh$" is computed for debris flow according to the following simple formula, which averages the movement of all the mass as the barycenter movement of a body on a constant slope with a constant friction coefficient:

$$sh = v\cdot t + g\cdot(\sin\theta - fca\cdot\cos\theta)\cdot t^2/2 \quad (12)$$

with "$g$" the gravity acceleration, the initial velocity

$$v = \sqrt{(2g\cdot KH[0])} \quad (13)$$

The motion involves three possibilities: (a) only internal flow, i.e., the shifted cylinder is completely inside the central cell; (b) only external flow, all the shifted cylinder is inside the adjacent cell; (c) the shifted cylinder is partially internal to the central cell, partially external to the central cell, the flow is divided between the central and the adjacent cell, forming two cylinders with barycenters corresponding to the barycenters of the internal debris flow and the external debris flow. The

kinetic head variation is computed according to the new position of internal and external flows, while the energy dissipation was considered as a turbulence effect in the previous elementary process.

- **Flows Composition**

When debris outflows are computed, the new situation involves that external flows left the cell, internal flows remain in the cell with different co-ordinates and inflows (trivially derived by the values of external flows of neighbor cells) could exist. The new value of *TH* is given, considering the balance of inflows and outflows with the remaining debris in the cell. A kinetic energy reduction is considered by loss of flows, while an increase is given by inflows: the new value of the kinetic head is deduced from the computed kinetic energy. The co-ordinates determination is calculated as the average weight of *X* and *Y* considering the remaining debris in the central cell, the internal flows and the inflows.

### *C. Simulation with SCIDDICA-SS2*

The SCIDDICA-SS2 was calibrated using the 1997 Albano lake (Italy) debris flow that is a case of combined subaerial-subaqueous event and validated with other five cases occurred on the lake slope [22]. This landslide is happened in the eastern slope of the Albano Lake on the November 7, 1997, after an intense rainfall event, mobilizing about 300 $m^3$ of alluvial material. Simulations permit to validate the general model and to calibrate adequately its parameters [21], [11]. Fig. 1 shows the corresponding simulation concerning subaerial/subaqueous part.

SCIDDICA-SS2 model was also used for a preliminary evaluation of the spatial hazard in the same area [23]: 89 hypothetical debris-flows, including 11 subaqueous ones, were simulated. Hypothetical sources are located at the vertices of a square grid with side length 50 m. A simple scene susceptibility (Fig. 2) was generated in a GIS (Geographic Information System) overlaying the paths of simulated flows, both subaerial that subaqueous.

## IV. The Model SCIDDICA-SS3

One of the latest models of the SCIDDICA family, named SCIDDICA-SS3, inherits all the features of its predecessor SS2 version, in order to improve management of physical conservation laws, in particular, inertial effects that characterize some rapid debris flow [12].

### *A. New features of SCIDDICA-SS3*

In the SS3 version of SCIDDICA, a better approximation has been introduced for the determination of outflows from a cell towards its adjacent cells, in terms of momentum computation.

The following sub-states $S_{Mx}$ and $S_{My}$, the two components of the debris momentum, are added.

The main difference consists in determination of a further alteration of data regarding the height values; directional effects concerning momentum are expressed by a correction function *corr*, which diminishes the height for cells in the same direction of the momentum and increases the height for cells in the opposite direction. It is applied to computation of minimizing outflows:

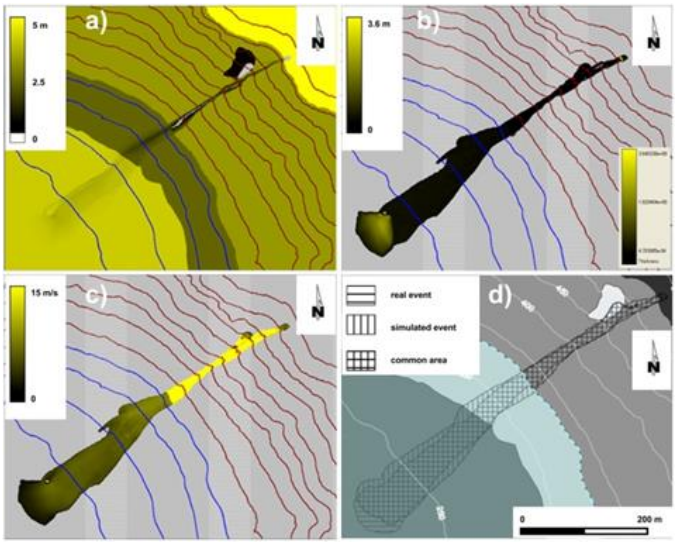


Fig. 1 Simulation of 1997 Albano Lake debris flow. (a) eroded regolith; (b) final thickness; (c) maximum local velocities reached by simulated flows; (d) real event compared with SCIDDICA-SS2 simulation

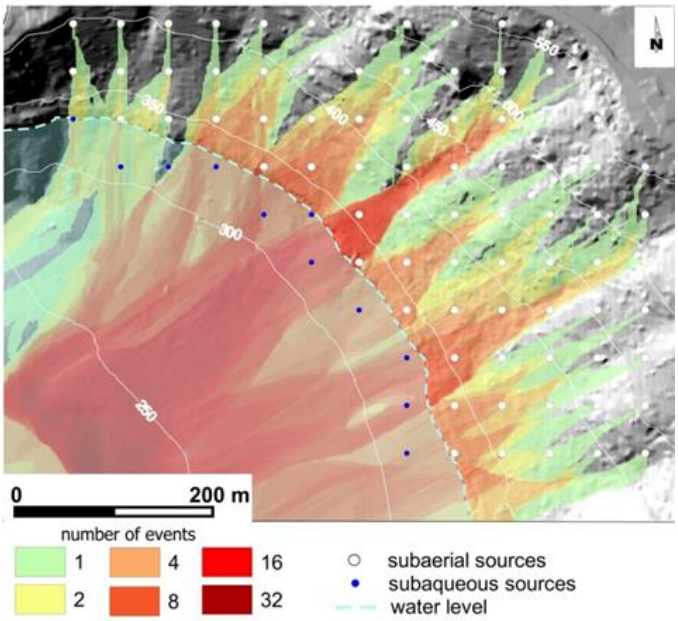


Fig. 2 Albano lake susceptibility zonation

$$h[0] = A[0] + KH[0] + adh \quad (14)$$

$$h[i]=A[i]+TH[i]+corr(Mx[0],My[0]), \quad (1\leq i\leq 6) \quad (15)$$

$$q = TH[0] - adh = \Sigma_{0\leq i\leq 6}\, f[i] \quad (16)$$

Trivial changes of momentum are computed in elementary processes involving energy loss: turbulence effect and mobilization effect.

### *B. Simulation with SCIDDICA-SS3*

SCIDDICA-SS3 version was applied for simulating 2009 debris flows in Giampilieri Superiore in Messina city territory.

On October 1, 2009, almost all the Peloritani Mountains area (NE Sicily) was involved in a rainfall (approximately 17 cm of rain in 180 minutes) with more than 500 landslides.

Fig. 3 shows a good simulation of debris flows that describe the debris run-out, especially in high zone of slope. Hence, such results may be a base for evaluating debris flow hazard and effects of possible remedial works in this study area [24], [25] and in other area with similar geophysical features.

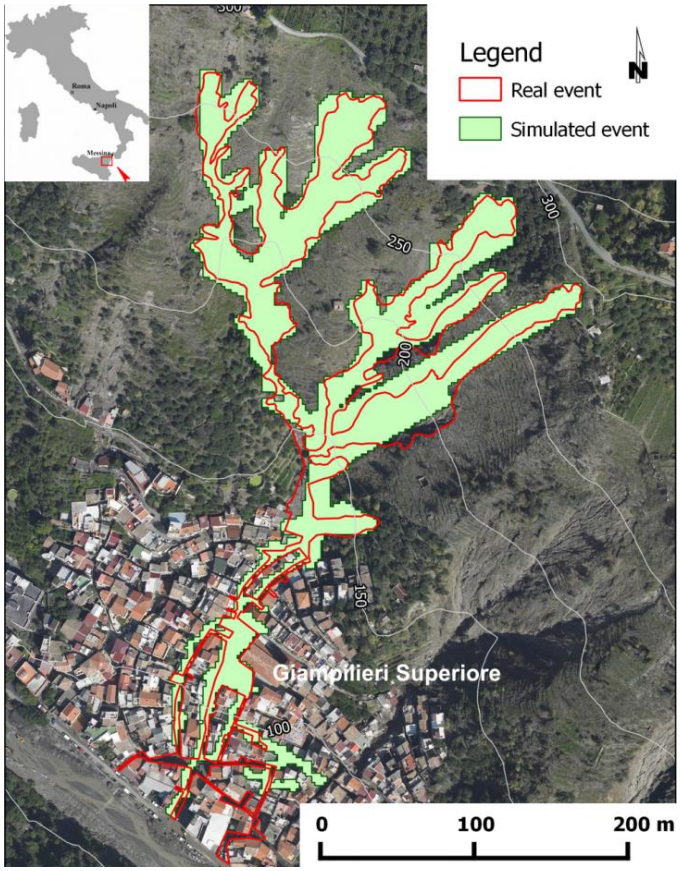


Fig. 3 Giampilieri Superiore debris flow compared with SCIDDICA-SS3 simulation

In order to validate SCIDDICA SS3 model the same set of parameters used to reproduce Sopra Urno debris flow, was used to simulate the other five debris flow run-out in the nearby catchments [24], [25] (Fig. 4). In all considered cases, the fitness function (5) return values between 0.70 and 0.78 (Table III), and the path of the flows is adequately reproduced.

Table III value of fitness function in considered location

| *case* | *R ($m^2$)* | *S ($m^2$)* | f |
|---|---|---|---|
| **a** | 11785.76 | 15924.21 | 0.73 |
| **Giampilieri debris flow** | 19476.87 | 28066.64 | 0.74 |
| **b** | 14168.38 | 22374.40 | 0.77 |
| **c** | 9207.63 | 17049.25 | 0.70 |
| **d** | 3768.42 | 6936.00 | 0.72 |
| **e** | 8934.52 | 13667.88 | 0.78 |

A pre-event a DEM was not available for these cases and the simulations were based on a pre-event DTM (i.e., without the buildings). In fact, it is possible to note how the flows are not influenced by presence of buildings in inhabited center (Fig. 4(b) and 4(c)). For cases (a), (d) and (e) (Fig. 4) the problem not is relevant because in these areas there are not buildings.

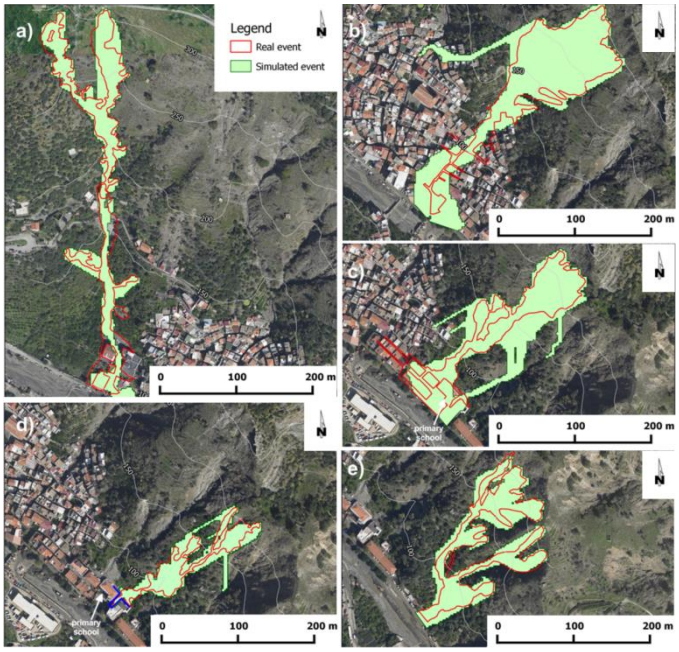


Fig. 4 Comparison between real debris flows and simulated events

The SCIDDICA-SS3 model, calibrated and validated on Giampilieri debris flows, was applied in order to produce susceptibility scenarios in the areas around A18 highway, Messina Sud tollgate, which presented similar soil characteristics and morphological conditions of slopes. This is a necessary condition in order to apply in other areas the SCIDDICA-SS3 validated parameters.

The carriageway is protected by a wall high about 1.50 m, in correspondence of the tollgate is located a drainage channel that interrupts the continuity of the wall (Fig. 5).


Fig. 5 View of Messina Sud tollgate area of A/18 highway

This introduces a source of risk for the highway. In fact, the tollgate area has been interested several times by debris inundation, due also to lack of appropriate maintenance of the channel. In fact, boulders and/or shrubs ripped along the path, from the flows, could obstruct the channel favoring the overflow of debris.

A pre-event DEM with 2 m cell size and for debris cover a uniform thickness of 0.5 m was used for simulation. This value seems to produce results that are consistent with the frequency of observed events.

Sources were identified for debris flow triggering return period of 4 and 5 years. These are obtained through the areas of probable detachments, i.e., analysis of precipitation for the determination of the rainfall Intensity-Duration-Frequency curves (IDF) [26], [27], [28]. In particular, the probabilistic rainfall analysis provides the rainfall input scenarios of different return periods, which are then used as input [28] to a model based of the USGS TRIGRS model to determine the corresponding trigged areas. TRIGRS [29], [30] developed for analyzing shallow landslide triggering is based on an analytical solution of linearized forms of the Richards' infiltration equation and an infinite-slope stability calculation to estimate the timing and locations of slope failures.

In Fig. 6(a) and (b) the results of simulations are shown, respectively for return period of 4 years and 5 years. Simulations show that the flow is channeled and the debris invades the highway carriageway at the lowest point of the morphology, i.e., the drainage channel (Fig. 6(a) and (b)).

In order to verify whether the presence of a higher wall could prevent the invasion of the highway it was included in DEM a topographical alteration along the previous wall that is raised by 2 m. The added wall is imposed as "indestructible" in our simulations. Fig. 6(c) and (d) show the results of the simulations for the same return periods; such scenarios account for topographical alteration. The simulations show that such a wall is able to stem the flow completely for 4 years return period avoiding highway invasions and/or damage, while only small quantities of debris overcome the wall at the lowest point in the case of 5 years return period.

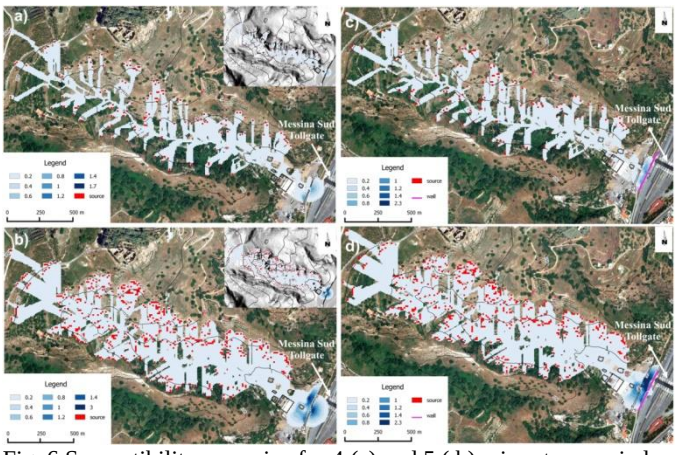

Fig. 6 Susceptibility scenarios for 4 (a) and 5 ( b) rain return period; in (c) and (d) scenartious with insertion of a wall

## V. The Model LLUNPIY

Submission Lahars are very complex dynamical systems, very difficult to be modelled: they can grow by soil erosion and/or incorporation of water, along watercourses. Unconsolidated pyroclastic material can be easily eroded by superficial water forming dilute sediment-laden flows, which can bulk-up to debris flows whose magnitude will depend upon the volume of both the water and remobilized material. Volcanic eruptions can generate directly (primary lahars) or indirectly (secondary lahars) catastrophic surface flows that are a mixture of volcanic debris and water occurring on and around volcanoes [13].

LLUNPIY (**L**ahar modelling by **L**ocal rules based on an **UN**derlying **PI**ck of **Y**oked processes, from the Quechua word llunp'iy meaning flood) is a CA model for simulating primary and secondary lahars in terms of complex system evolving on the base of local interaction. This model inherits all the features of SCIDDICA-SS2 [21], [11].

### *A. Formal definition of LLUNPIY*

SCIDDICA-SS3 The LLUNPIY model is a two dimensional CA with a hexagonal tessellation and is defined by the septuplet:

$$<R, G, X, S, P, \tau, \gamma>$$

where:

- $R = \{(x, y): x, y \in \mathbb{N}, 0 \le x \le l_x, 0 \le y \le l_y\}$ is the set of points with integer co-ordinates, that individuate the regular hexagonal cells;
- $G \subseteq R$ is the set of cells, corresponding to the glacier, where lahar is formed when pyroclastic matter melts ice (the case of primary lahars) or cells effected by rainfall (the case of secondary lahars);
- $X$ = {(0, 0), (1, 0), (0, 1), (−1, 1), (−1, 0), (0,−1), (−1,−1)}, the neighbourhood index, identifies the geometrical pattern of cells, which influence state change of the "central" cell;
- $S$ is the finite set of states of the finite automaton, embedded in the cell; it is equal to the Cartesian product of the sets of the considered sub-states (Table IV).
- $P$ is the set of the global physical and empirical parameters, which account for the general frame of the model and the physical characteristics of the phenomenon (Table V);
- $\tau: S^7 \rightarrow S$ is the cell deterministic state transition in R, it embodies the SCIDDICA-SS2 elementary processes, furthermore introducing two new ones in order to account to characteristics of the lahar dynamics: the following main components of the phenomenon:
  - $\sigma_{wp}$, water percolation;
  - $\sigma_{psm}$, pyroclastic stratum mobilization;
  - $\sigma_{wf}$, water flow;
  - $\sigma_{wie\&ld}$, water inclusion, extrusion and process of lahar complete deposition
- $\gamma_1$: $\mathbb{N}\times G_g\times S_{IT}\times S_A\times S_{LT} \rightarrow S_{IT}\times S_A\times S_{LT}$ for primary lahars expresses the "external influence" of fall of the pyroclastic matter on glacier ($G_g$ cells) and consequently ice state change in lahar with the addition of pyroclastic matter at the initial CA step. $\mathbb{N}$ is here referred to the step number.
- $\gamma_2$: $\mathbb{N}\times G\times S_{WL}\times S_{WKH} \rightarrow S_{WL}\times S_{WKH}$ for secondary lahars expresses the raining water quantity to be added

for *G* cells at each CA step. ℕ is here referred to the step number.

Table IV Sub-states

| *Sub-States* | *Description* |
|---|---|
| $S_A$, $S_{D,}$ ($S_{D1}$, $S_{D2}$) | cell **A**ltitude, tephra stratum **D**epth; it could be specified if data are available in "**1**" the mobilizable stratum, and "**2**", the only erodible stratum. |
| $S_{SR}$, $S_{SWC}$, $S_{MIR}$ | mobilizable stratum: **S**tratum **R**eceptivity, **S**tratum **W**ater **C**ontent, **M**ax **I**nfiltration **R**ate |
| $S_{WL}$, $S_{WKH}$, $S_{WO}$ | **W**ater **L**evel, **W**ater **K**inetic **H**ead, **W**ater **O**utflows (6 components normalized to a thickness) |
| $S_{IT}$ , $S_{LT}$, $S_{KH}$, $S_{LWC}$ | **I**ce **T**hickness**,** **L**ahar **T**hickness, Lahar **K**inetic **H**ead, **L**ahar **W**ater **C**ontent |
| $S_X$, $S_Y$ | the co-ordinates **X** and **Y** of the lahar barycenter inside the cell |
| $S_{MX}$, $S_{MY}$, | the components **x** and **y** of the lahar **M**omentum inside the cell |
| $S_E$, $S_{EX}$, $S_{EY}$, $S_{KHE}$ (6 components) | **E**xternal flow normalized to a thickness, **E**xternal flow co-ordinates **X** and **Y**, **K**inetic **H**ead of **E**xternal flow |
| $S_I$, $S_{IX}$. $S_{IY}$, $S_{KHI}$ (6 components) | **I**nternal flow normalized to a thickness, **I**nternal flow co-ordinates **X** and **Y**, **K**inetic **H**ead of **I**nternal flow |

Table V Physical and empirical parameters

| Parameters | Description |
|---|---|
| $p_a$ $p_t$ | cell **a**pothem, **t**emporal correspondence of a CA step |
| $p_{fc}$ | **f**riction **c**oefficient parameter |
| $p_{td}$ $p_{ed}$ $p_{pe}$ $p_{mt}$ | lahar parameters: **t**urbulence **d**issipation and **e**rosion **d**issipation of energy; lahar parameter of **p**rogressive **e**rosion, **m**obilization **t**hreshold |
| $p_{slt}$ $p_{wct}$ | slope threshold, **w**ater **c**ontent **t**hreshold |
| $p_{khl}$ | **k**inetic **h**ead **l**oss |
| $p_{dft}$ $p_{adh1}$ $p_{adh2}$ | lahar complete **d**eposit **f**ormation **t**hreshold, minimum **adh**erence, maximum **adh**erence |

*B. The specific LLUNPIY elementary processes*

- **$\sigma_{wp}$, water percolation:** part of water from rainfall infiltrates in the mobilizable stratum, that may be considered as a water reservoir of a given capacity, that is the sum of stratum water receptivity $S_{SR}$ plus stratum water content $S_{SWC}$; a maximum infiltration rate (in a step) $S_{MIR}$ is fixed according to the cell physical characteristics related to the mobilizable stratum. Infiltration $v_I$ is the minimum value among $S_{WL}$, $S_{SR}$ and $S_{MIR}$. Sub-states are updated:

$$S_{WL}' = S_{WL} - v_I \quad S_{SR}' = S_{SR} - v_I \quad S_{SWC}' = S_{SWC} + v_I$$

- **$\sigma_{psm}$, pyroclastic stratum mobilization:** the saturation conditions of pyroclastic stratum are specified by overcoming two thresholds, that regard the percent of $S_{SWC}$ related to water capacity of the mobilizable stratum and a sufficient slope angle $\alpha_i$ related to some adjacent cell $i$ $(1 \le i \le 6)$ such that the slope component of gravity force is larger than the reduced cohesion forces:

$$S_{SWC} / (S_{SWC} + S_{SR}) > p_{wct} \quad \arctan(\alpha_i) > p_{slt}$$

When saturation conditions occur, the mobilizable stratum liquefies after the collapse of soil cohesion forces and encloses the surface water; then:

$$S_{LT}'=S_{D1}+S_{WL}-S_{SR};\ S_{LWC}'=(S_{SWC}+S_{WL})/(S_{D1}+S_{WL}-S_{SR});$$
$$S_{WL}'=S_{SR}'=S_{D1}'=0;\ S_A'=S_A-S_{D1}$$

- **$\sigma_{wf}$, water flow:** outflows are computed by the simplest application of AMD.

- **$\sigma_{wie\&ld}$, water inclusion, extrusion and process of lahar complete deposition:** when $p_{slt}<S_{KH}<p_{wct}$, water extrusion occurs, according an empirical approximate function "water loss": $\Delta S_{LWC} = f_{wl}(S_{KH}, p_{slt}, p_{wct})$, $f_{wl}$ accounts for water extrusion in lahar and expresses linearly water content loss between two values of kinetic head $p_{slt}$ and $p_{wct}$, considering that gravitational water content at $p_{slt}$ is approximated to 0. When $S_{KH} \le p_{slt}$ lahar stops and complete deposition occurs: $\Delta S_A = S_{LT}$; $S_{LT}' = 0$; $S_{LWC}' = 0$, in the case of secondary lahars, intrusion of all the water of rainfall into the lahar is considered when $S_{KH} > p_{wct}$, $S_{LWC}$ and $S_{LT}$ increase proportionally to intruded water.

*C. Simulation with LLUNPIY*

- **Secondary lahars: 2008 Tungurahua volcano case of study**

Tungurahua volcano is located in the Cordillera Oriental of Andes of central Ecuador. With its elevation of 5023 m a.s.l., the volcano has tremendous relief over the surrounding landscape. The city of Baños is located on the northern flank of the volcano at an elevation of 1800 m, some 3200 m below the summit crater. In the last 15 years around 900 rain-induced lahars were generated. Thanks to Instituto Geofísico of the Escuela Politécnica Nacional (IGEPN) that uses acoustic-flow-monitor (AFM) station to detect and register secondary lahar activity, most lahars were detected, and others were observed by OVT (Observatory Volcanic Tungurahua) located 13 km north-northwest of the crater and also by "vigias" (local volunteer volcano observes). On August 2008 the Vascún valley was interested by frequent and mostly heavy rainfall [31].

On 13 August, a 13 mm rainfall in three hours caused a small landslide that generated a natural barrier along Rio Vascún at an altitude approximately of 2200 m a.s.l. The barrier created at upstream a pond 3 m deep, 20 m wide and with a length 100 m; the saturation of tephra deposits in that area because of persistent rainfalls caused on August 22 the collapse of barrier and generated a lahar [31]. Such a lahar may be considered secondary because its dynamics involve mechanisms that are typical of the previous secondary lahars in the area. This justifies the use in simulation of the same

values of parameters of 2005 event. The documentation does not report any information about lahar volume.

The simulation of 2008 event is based on DEM with 1m cell size with vertical accuracy from 0.6 m to 1.3 m (supplied to us by Dr. Gustavo Cordoba). It was integrated (in QGIS software) for the last 500 m by a DEM with 5 m cell size (supplied to us by IGEPN). Also, a uniform thickness of 5m was imposed for detrital cover, because detailed surveys were not available. All this introduces a series of approximations that affects certainly simulations but do not detract from the effectiveness of the model. Simulations regard the flood phase of the events (elementary processes: "soil erosion" "lahar thickness and outflows" with an appropriate simplification about the moment computation, that shorten computation times.

Fig. 7(a) shown the 2008 lahar simulation: the flow velocity reaches, in many areas of the valley, 20 m/s (Fig. 7(b)) with a total of eroded material (Fig. 7(c)) of about 970000 $m^3$. In table VI is reported comparison between field data, collected by IGEPN [31], and LLUNPY simulation data.

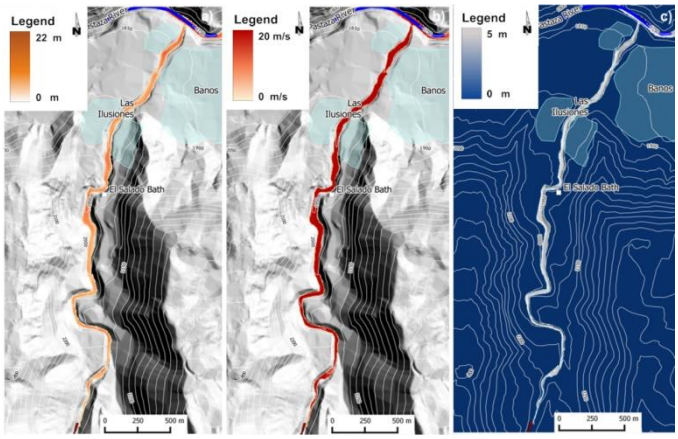


Fig. 7 (a) Maximum thickness, (b) Maximum velocity, and (c) erosion depth, in simulated event

A partial simulation of the first phase of the event (only detachment) was performed by a reduced two-dimensional CA "ad hoc" in order to compare experimental scarce data about triggering areas, which we adopted in the simulation, and data, that are obtained by application of the combined elementary processes: water percolation, water flow, pyroclastic stratum mobilization. The Vascún Valley may be considered a canyon for the lahars, so linearizing the path in only two dimensions doesn't involve serious problems of approximation in order to implement the partial CA. The soil (tephra) data were considered almost homogeneous in terms of composition; such an assumption is critical, because soil tomography data [32] show heterogeneity that we averaged. In spite of this weak point, triggering areas of simulation agree with experimental data. In simulation we consider two meters of saturable tephra with voids content of 35%.

Fig. 8 reports the elevation profile of the lahar path as a colored band of constant thickness, whose color represents the degree of water content. The overlying blue and brown zones represent the water and lahar thickness (not in scale). Green zones interposed to brown zones in Fig. 8(b) represent collapsed tephra together the water inside. Fig. 8(a) show water accumulation points (blue peaks), along the Vascún Valley, after 14 hours of and intense rainfalls (28.8 mm/h). Soil saturation is maximum after 19 hours. Triggering of lahars (green zones in Fig. 8(b)) occurs in many points after about 20 hours of continue rain with the same intensity, where soil conditions allow (e.g., saturation, slope angle, etc.). Note the correspondence between the source areas of the events occurred in 2005 and in 2008, respectively at elevation of 4090 m a.s.l. and 2200 m a.s.l.

Table VI Comparison between field data and LLUNPIY simulation data

| | ***Field data*** | ***LLUNPIY Simulation data*** |
|---|---|---|
| Maximum velocity | 15 m/s | 20 m/s |
| Velocity at El Salado | 4.7 m/s | 6 m/s |
| Time between start point and El Salado | 5' | 4' 50" |
| Maximum flow between start point and El Salado | 640 $m^3$/s | 633 $m^3$/s |
| Total time between start point and Rio Pastaza | - | 9' |
| Total eroded debris | - | 970000$m^3$ |

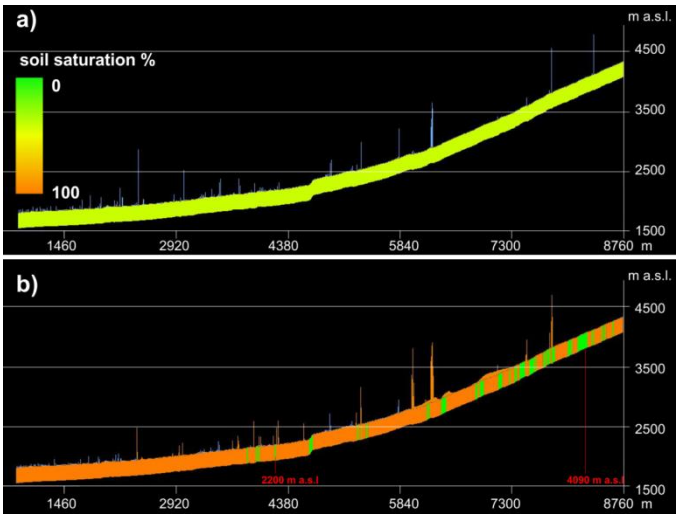


Fig. 8 A two-dimensional CA for determination of possible triggering points. (a) Blue peaks represent water accumulation points, (b) green zones are possible triggering points of lahars, brown peaks are points of detrital accumulation. Red altitudes evidence the triggering points of real past events that coincide with some green bands

- **Primary lahars: 1877 Cotopaxy volcano case of study**

Cotopaxi is a potentially active stratovolcano in the Andes Mountains, located about 50 km south of Quito, Ecuador, South America. The main danger of a huge eruption of Cotopaxi would be the flow of ice from its glacier with pyroclastic material. In the case of large eruption, it could destroy many settlements around the volcano. One of these is the city of Latacunga, which is located in the south-west

valley and already destroyed in the 18th century (a village at that time) by volcanic activity [33], [34].

LLUNPIY model was applied to Cotopaxi 1877 event of primary lahars [33], after the successful simulation of some secondary lahars of Tungurahua volcano [14], [35]. We followed, as first approach, the "many sources" simplification proposed in Pistolesi et al. [34] that the main event could be equivalently generated, considering the initial positions of lahars sources in the three principal streams (Fig. 9): Río Cutuchi, Río Sasqìmala and Río Barrancas-Alaques. In each of these three streams, we have placed, respectively, $18.5 \times 10^6$ m$^3$, $9.5 \times 10^6$ m$^3$ and $10 \times 10^6$ m$^3$ of lahar matter.

The resultant simulations are shown in Fig. 9. These results are comparable with simulations performed by the model LAHARZ [34], that considered larger quantities of initial lahars ($120 \times 10^6$ m$^3$ sum of: $60 \times 10^6$ m$^3$ in Río Cutuchi, $30 \times 10^6$ m$^3$ in Río Sasqímala and $30 \times 10^6$ m$^3$ in Río Barrancas-Alaques). The width of LLUNPIY simulation is smaller in the area next to "spurious" sources, but LAHARZ simulation is larger (Fig. 9). The two results are very similar in the final sector (Latacunga area), because, at the end, the addition of eroded material in LLUNPIY balances the two approaches.

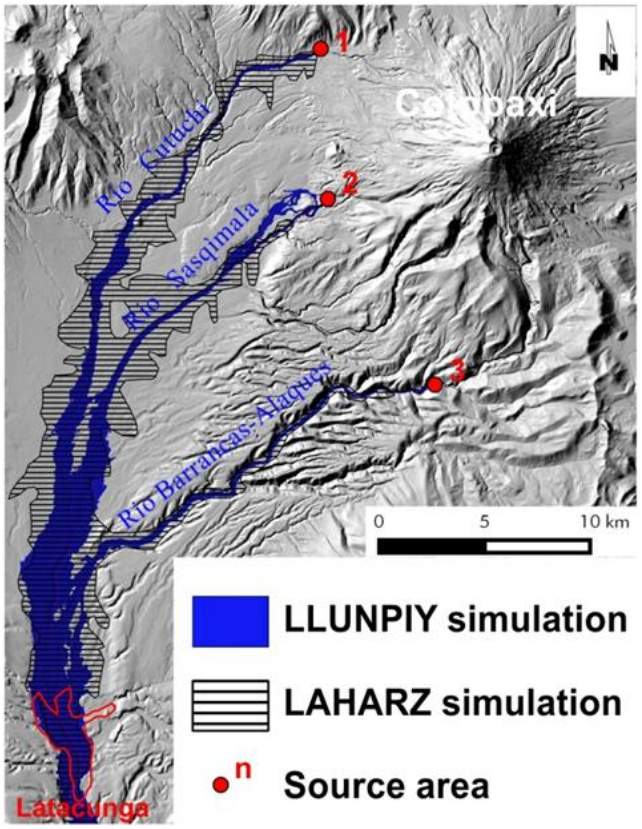


Fig. 9 LUNPIY "many sources" simulation of 1877 lahars

This CA approach involves the limit of initial quantity of lahar at the sources, because overflows can distort the effective evolution of the phenomenon. This did not permit to overcome an initial lahar quantity at the beginning in the previous simulation. For this purpose, we introduce a new CA "elementary process" of glacier melting. The ice layer is supposed to enclose pyroclastic matter and to melt immediately (the LLUNPIY first step) the glacier. That is more realistic of the "many Sources Approach" than sources approach, if the rapid evolution of eruption is considered. The simulations of icecap melting are based on data, which correspond to 1976 glacier extension [36] with average glacier thickness of 50 m. In the simulation, only 10m of ice is melt. Fig. 11 shows the results of simulated event in various times. The paths are the same of "many source" simulation, but in the case of "glacier melting" widths are obviously larger. Results of simulation agree with partial data of the chronicles of that time [37]. Such a simulation could be considered a possible scenario for a future eruption of Cotopaxi because current DEM (Digital Elevation Model) was used together with measures of glacier extension.

In the simulations, we have considered two possible scenarios. The first case involves the melting of only 10m of glacier [38]. Fig. 10 shows the results of simulated event in various times. A second scenario (Fig. 11), more catastrophic, involves the complete melting of ice cap. In this case the flows enlarge, covering a more extensive area in larger times. In both cases the paths are the same of "many source" simulation, but in the case of "glacier melting" widths are obviously larger. Results of simulation agree with partial data of the chronicles of that time [37]. These simulations could be considered possible scenarios for a future eruption of Cotopaxi because current DEM (Digital Elevation Model) was used together with measures of glacier extension.

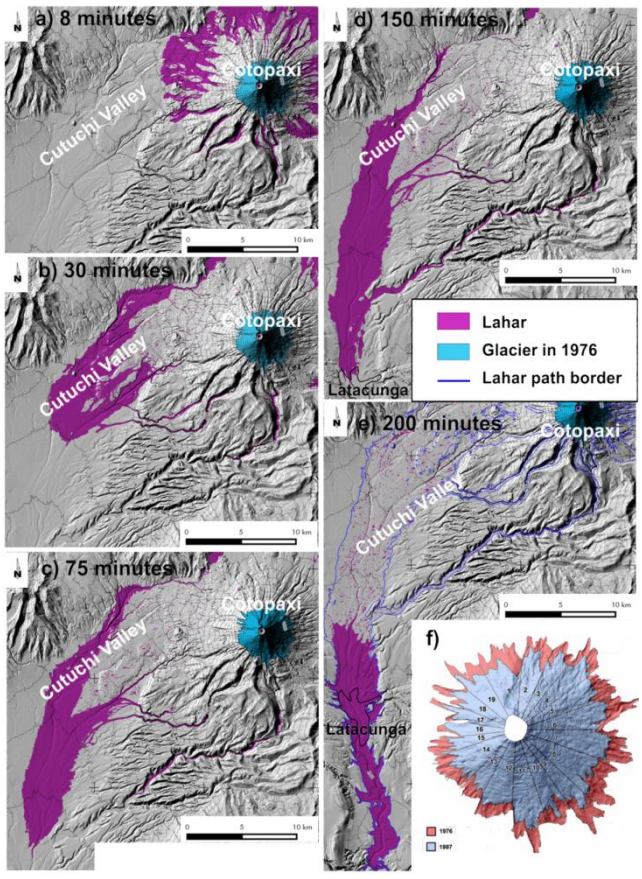


Fig.10 LLUNPIY scenario 1 considering 10 m of ice cap melting

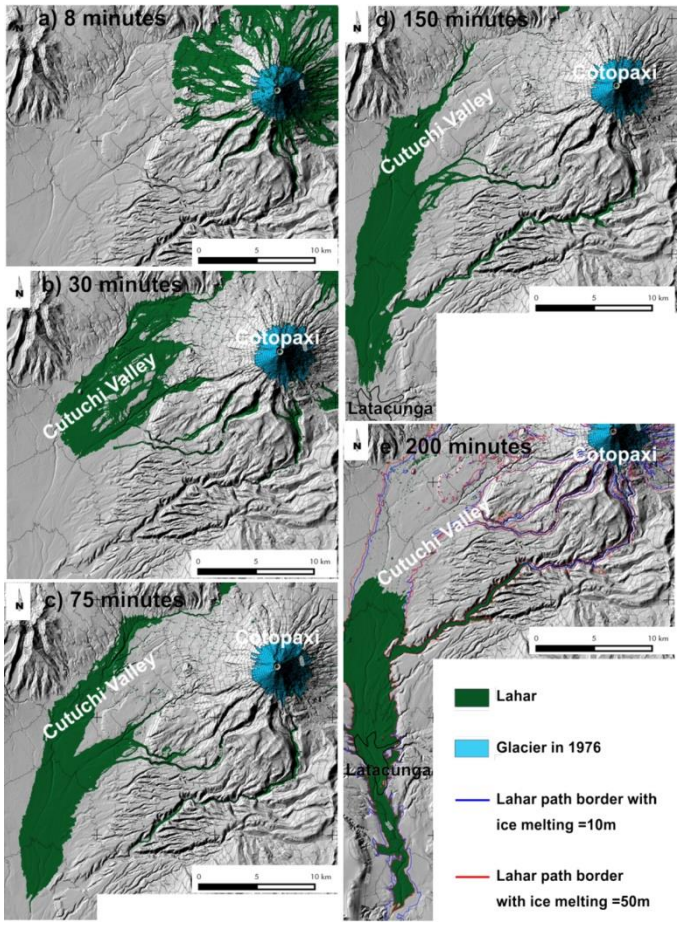


Fig. 11 LLUNPIY scenario 2 considering 50 m of ice cap melting

## VI. Conclusion

The MCA methodological approach was applied in order to develop models of different fast moving surface flows of the type lahar and debris flow. Such models, SCIDDICA-SS2, SCIDDICA-SS3 and LLUNPIY present a similar structure that is differentiated in relation to the characteristics of the phenomenon; it implies the introduction of different and/or new elementary processes together with new sub-states and parameters. The common core regards the calculation of moving quantities from the central cells to the other cells of the neighboring; such outflows are idealized as "cylinders" tangent the next edge of the own hexagonal cell, according different motion equations; the different formulae based on the minimization algorithm determine quantity and direction of the outflows. MCA approach allows easily to introduce new elementary processes for refining or differentiating CA models.

SCIDDICA-SS3 represents a SCIDDICA-SS2 extension for cases, where a better approximation of momentum is necessary; in fact, some elementary processes were expanded.

LLUNPIY introduces new elementary processes that permitted to adequate the "common" elementary processes to lahar features and to introduce various triggering mechanisms that yielded to the new satisfying results concerning the 1877 lahars of Cotopaxi volcano, starting from simulation of the immediate melting of part of the Cotopaxi icecap.

Future research about lahar will continue with improving the triggering process, by considering the progressive glacier melting by pyroclastic bombs of volcanic eruptions for the Cotopaxi case.

## References

[1] J. von Neumann, "Theory of self-reproducing automata". Edited and completed by Arthur W. Burks. Illinois University Press, 1966.
[2] B. Hayes, "The cellular automaton offers a model of the world and a world unto itself". Scientific American, 250(3), 1984, pp.12–21.
[3] D. Barca, S. Di Gregorio, F.P. Nicoletta, M. Sorriso-Valvo, "A cellular space model for flow type landslides". In Computers and their Application for Development. Proc. Int. Symp. IASTED (Taormina). 1986. pp. 30–32.
[4] S. Di Gregorio, R. Serra, "An empirical method for modelling and simulating some complex macroscopic phenomena by cellular automata". Future Generation Computer Systems Vol.16, No2/3, 1999, pp. 259-271.
[5] M.V. Avolio, S. Di Gregorio, V. Lupiano, P. Mazzanti, W. Spataro, "Application context of the SCIDDICA model family for simulations of flow-like landslides". In Proceedings international conference on scientific computing, Las Vegas (USA), 2010a, pp. 40–46.
[6] G.M. Crisci, S. Di Gregorio, R. Rongo, W. Spataro, "PYR: a Cellular Automata model for pyroclastic flows and application to the 1991 Mt. Pinatubo eruption". Future Generation Computer Systems, vol. 21, no 7, 2005, pp. 1019–1032.
[7] G.M. Crisci, M.V. Avolio, B. Behncke, D. D'Ambrosio, S. Di Gregorio, V. Lupiano, M. Neri, R. Rongo, W. Spataro, "Predicting the impact of lava flows at Mount Etna, Italy". J. Geophys. Res., Vol. 115, 2010, pp 1–14.
[8] M. V. Avolio, A. Errera, V. Lupiano, P. Mazzanti, S. Di Gregorio "Development and calibration of a preliminary Cellular Automata Model for Snow Avalanches". In Lecture Notes in Computer Sciences – Proceedings of ACRI 2010, Ascoli Piceno (Italy), 6350, 2010b pp. 83–94.
[9] A. Clerici, S. Perego, "Simulation of the Parma River blockage by the Corniglio landslide (Northern Italy)". Geomorphology, vol. 33, no 1, 2000, pp. 1–23.
[10] T. Salles, S. Lopez, M.C. Cacas, T. Mulder, "Cellular automata model of density currents. Geomorphology", Vol.88, 2007, pp. 1-20.
[11] M.V. Avolio, V. Lupiano, P. Mazzanti, S. Di Gregorio, "An advanced Cellular Model for Flow-type Landslide with Simulations of Subaerial and Subaqueous cases", Proceedings of 23rd EnviroInfo, Vol.1, Shaker Verlag, Aachen, 2009, pp. 131–140.
[12] M.V. Avolio, V. Lupiano, P. Mazzanti, S. Di Gregorio, "SCIDDICA-SS3: A New Version of Cellular Automata Model for Simulating Fast Moving Landslides", J. Supercomput., Vol. 65, 2013, pp. 682–696.
[13] G. Machado, V. Lupiano, M.V. Avolio, S. Di Gregorio, "A Preliminary Cellular Model for Secondary Lahars and Simulation of 2005 Case of Vascún Valley, Ecuador". In Proceeding ACRI 2014 International Conference, LNCS 8751 Springer International Publishing, 2014, pp. 208–217.
[14] G. Machado, V. Lupiano, M.V. Avolio, F. Gullace, S. Di Gregorio, "A cellular model for secondary lahars and simulation of cases in the Vascún Valley, Ecuador". J. Comput. Sci. 2015b, http://dx.doi.org/10.1016/j.jocs.2015.08.001.
[15] U. Frisch, D. D'Humieres, B. Hasslacher, P. Lallemand, Y. Pomeau, J.P. Rivet, "Lattice gas hydrodynamics in two and three dimensions". Complex Systems 1, 1990, pp. 649–707.
[16] B. Chopard, "Cellular automata modeling of physical systems". Computational Complexity: Theory, Techniques, and Applications, 2012, pp. 407–433.
[17] S. Succi, "The Lattice-Boltzmann Equation". Oxford university press, Oxford, 2001.
[18] M.V. Avolio, G.M. Crisci, D. D'Ambrosio, S. Di Gregorio, G. Iovine, R. Rongo, W. Spataro, "An extended notion of Cellular Automata for surface flows modelling". WSEAS Transactions on Computers, Vol. 4(2), 2003, pp. 1080–1085.
[19] M.V. Avolio, S. Di Gregorio, W. Spataro, G.A. Trunfio, "A Theorem about the Algorithm of Minimization of Differences for Multicomponent Cellular Automata". In ACRI 2012, LNCS 7495, Springer-Verlag Berlin, 2012, pp. 279–288.

[20] D. D'Ambrosio, S. Di Gregorio, S. Gabriele, R. Gaudio, "A Cellular Automata Model for Soil Erosion by Water". Physics and Chemistry of the Earth, Part B: Hydrology, Oceans and Atmosphere, vol. 26, no 1, 2001, pp. 33–39.
[21] M.V. Avolio, V. Lupiano, P. Mazzanti, S. Di Gregorio, "Modelling combined subaerial-subaqueous flow-like landslides by Cellular Automata". In Cellular Automata. Springer Berlin Heidelberg, 2008, pp. 329–336.
[22] P. Mazzanti, Bozzano F., Avolio M.V., Lupiano V., Di Gregorio S., "3D numerical modelling of submerged and coastal landslides propagation". Advances in Natural and Technological Hazards Research, Vol.28, Springer Verlag, Berlin, 2010. pp. 127–138.
[23] V. Lupiano, M. V. Avolio, M. Anzidei, G.M. Crisci, S. Di Gregorio, "Susceptibility Assessment of Subaerial (and/or) Subaqueous Debris-Flows in Archaeological Sites, Using a Cellular Model". In Engineering Geology for Society and Territory-Volume 8. Springer International Publishing, 2015, pp. 405–408.
[24] V. Lupiano, D. J. Peres, M. V. Avolio, A. Cancelliere, E. Foti, W. Spataro, L. M. Stancanelli, S Di Gregorio, "Use of the SCIDDICA-SS3 model for predictive mapping of debris flow hazard: an example of application in the Peloritani Mountains area". In Int'l Conf. Par. and Dist. Proc. Tech. and Appl. proceedings of PDPTA'15, Las Vegas, Nevada, USA. 2015, pp. 625–631.
[25] V. Lupiano, M. V. Avolio, S. Di Gregorio, D.J. Peres, L. M. Stancanelli, "Simulation of 2009 debris flows in the Peloritani Mountains area by SCIDDICA-SS3". In proceeding of 7th WSEAS International Conference on Engineering Mechanics, Structures, Engineering Geology, Salerno (Italy), 2014, pp. 53–61, ISBN: 978-960-474-376-6.
[26] L. M. Stancanelli, V. Bovolin, E. Foti, "Application of a dilatant - viscous plastic debris flow model in a real complex situation". River Coastal and Estuarine Morphodynamics, RCEM2011, Tsinghua University Press, Beijing, 2001, pp 45–64.
[27] L. M. Stancanelli, G. Rosatti, L. Begnudelli, A. Armanini, E. Foti, "Single or Two-Phase Modelling of Debris-Flow? A Systematic Comparison of the Two Approaches Applied to a Real Debris Flow in Giampilieri Village (Italy)". Landslide Science and Practice. 2013, doi: 10.1007/978-3-642-31310-3_37.
[28] L. M. Stancanelli, D. J. Peres, L. Cavallaro, A. Cancelliere, E. Foti, "Debris flow hazard assessment by integrated modeling of landslide triggering and propagation: application to the Messina Province, Italy". AGU Fall meeting Abstracts, 15-18 December 2014, San Francisco.
[29] R. L. Baum, W. Z. Savage, J. W. Godt, "TRIGRS – A FORTRAN program for transient rainfall infiltration and grid-based regional slope stability analysis, version 2.0.". US Geological Survey Open-File Report 2008-1159, pp. 1–75.
[30] R. L. Baum, W. Z. Savage, J. W. Godt, W. Z Savage, "Estimating the timing and location of shallow rainfall-induced landslides using a model for transient, unsaturated infiltration". Journal of Geophysical Research, Earth Surface, 2010, pp. 1–26. doi:10.1029/2009JF00132.
[31] IGEPN internal report, "Weekly Report from the Tungurahua Volcano Observatory. 18-24 August, 2008". Report No. 33 2008. Instituto Geofísico, Quito Ecuador. Available: www.igepn.edu.ec (Informes Volcánicos).
[32] E. Rizzo, (CNR IMAA - Institute of Methodology for Environmental Analysis, Italy) and S. Straface (Department of Environmental and Chemical Engineering, University of Calabria, Italy) (February 2015), personal communication.
[33] P. Mothes, J.W. Vallance, "Volcanic Hazards, Risks, and Disasters". In Lahars at Cotopaxi and Tungurahua Volcanoes, Ecuador, Elsevier Inc., New York, 2014, pp.141–167.
[34] M. Pistolesi, R. Cioni, M. Rosi, E. Aguilera, "Lahar hazard assessment in the southern drainage system of Cotopaxi Volcano, Ecuador: Results from multiscale lahar simulations". Geomorphology 207, 2014, pp. 51–63.
[35] G. Machado, V. Lupiano, G. M. Crisci and S. Di Gregorio, LLUNPIY "Preliminary Extension for Simulating Primary Lahars Application to the 1877 Cataclysmic Event of Cotopaxi Volcano". In SIMULTECH 2015, pp. 367–376.
[36] B. Cáceres, J. Ramírez, B. Francou, J.P. Eissen, J.D. Taupin, E. Jordan, L. Ungerechts, L. Maisincho, D. Barba, E. Cadier, R. Bucher, A. Peñafiel, P. Samaniego, P. Mothes, "Determinación del volumen del casquete de hielo del volcán Cotopaxi". Informe INAMHI, IRD, IG-EPN, INGEOMINAS, 2004.
[37] T. Wolf,, "Memoria sobre el Cotopaxi y su Última Erupción Acaecida el 26 de Junio de 1877". Imprenta del Comercio, Guayaquil, Ecuador, 1878.
[38] V. Lupiano, G. Machado, G. M. Crisci, S. Di Gregorio, "Modelling Fast-moving Flow-like Landslides by Cellular Automata: Simulations of Debris Flows and Lahars". In: Advances in Environmental and Geological Science and Engineering, proceeding of WSEAS 8th International Conference (EG '15), Salerno, Italy, 2015, pp 401–411.